Optimal low-thrust orbital transfer for servicing multiple satellites in elliptical orbits

Acta Astronautica 228 (2025) 686–699

Contents lists available at ScienceDirect

Acta Astronautica

journal homepage: www.elsevier.com/locate/actaastro

Research paper

Optimal low-thrust orbital transfer for servicing multiple satellites in elliptical orbits

Riccardo Apa [a,*], Isaac Kaminer [b], Jennifer Hudson [b], Marcello Romano [a]

[a] Department of Mechanical and Aerospace Engineering, Politecnico di Torino, Corso Duca degli Abruzzi 24, 10129, Turin, Italy
[b] Mechanical and Aerospace Engineering Department, Naval Postgraduate School, 1 University Cir, 93943, Monterey, CA, USA

ARTICLE INFO

Keywords:
Space trajectories
Traveling salesman problem
Low-thrust propulsion
Space logistics
Astrodynamics

ABSTRACT

This paper addresses the problem of finding the optimal sequence and trajectory for a servicer satellite that has to visit multiple client satellites, minimizing the fuel spent and satisfying Keplerian dynamics and low-thrust propulsion constraints. The cost of each transfer is evaluated through two different functions: an analytical cost function based on Edelbaum's theory (three orbital elements transfer), and a Q-law based cost function (five orbital elements transfer). The global optimal sequence is found by using mixed integer linear programming. The proposed methodology is demonstrated on two datasets of satellites located in near-circular and high-eccentricity orbits, respectively. The computation results show a high performance in terms of computational time and accuracy.

1. Introduction

On-orbit Servicing, Assembly, and Manufacturing (OSAM) missions [1] are drawing increasing attention. In particular, an OSAM mission to serve multiple satellites involves multiple rendezvous maneuvers between the servicing satellite and the client satellites. Problems of this kind, referred to as *"Moving-Target (or time-dependent) Traveling Salesman Problems"* (MTTSP), are Nondeterministic Polynomial-time complete (NP-complete) [2] and involve the choice of the optimal visiting sequence of the clients, which are subject to orbital dynamics (moving targets). A cost in terms of propellant, time, or a combination of the two [3] is associated with each individual visiting maneuver (leg); the optimal sequence coincides with the sequence whose total cost of all legs is the lowest possible. The optimization problem consists of a mixed integer/continuous variable problem. MTTSP can be split into the following two sub-problems [4]:

1. A combinatorial problem involving the generation of the sequence of clients to visit
2. A functional problem, where the cost of each maneuver (*distance metric* or *leg cost function*) is computed by solving an optimal control problem

The choice of the algorithms solving the above two problems is dependent on the orbital dynamics model used to propagate the satellites' trajectories, the servicer propulsion system characteristics, and the dataset size.

Several authors have presented solutions of MTTSP for the case of high-thrust propulsion system [3–7]. The GTOC-9 competition proposed a debris-removal mission of this type [5]. The winning team presented a solution to remove 123 debris objects. Ten different missions were required to remove all of the debris.

As an alternative strategy, low-thrust propulsion systems, as considered in this paper, allow for reduced fuel consumption for multiple-visitation missions.

In the context of low-thrust propulsion, solutions to MTTSP have previously been proposed [8–13]. These solutions make different assumptions regarding the perturbations included in the dynamics model, the number of orbital elements targeted, the servicer fuel mass depletion, constraints due to eclipse, optimization criteria (e.g., minimum-time or minimum-fuel), and the algorithm solving the combinatorial problem. In Ref. [8], the authors find the optimal sequence of a multiple-visitation problem by adopting a simple distance metric (only inclination and Right Ascension of the Ascending Nodes (RAAN) differences between satellites are considered) similar to that employed in Ref. [14]. The sequence so found is then propagated by a Rendezvous Q-law (RQ-law) in order to obtain fuel consumption and trajectories for a six-orbital-element targeting solution. However, importantly, the RQ-law is not employed as a distance metric to solve the combinatorial problem. In Ref. [9], the authors solve the combinatorial problem by adopting an analytic distance metric accounting for three-orbital-element targeting for minimum-time transfer. The approach considers

* Corresponding author.
E-mail addresses: riccardo.apa@polito.it (R. Apa), kaminer@nps.edu (I. Kaminer), jennifer.hudson@nps.edu (J. Hudson), marcello.romano@polito.it (M. Romano).

https://doi.org/10.1016/j.actaastro.2024.12.030
Received 30 September 2024; Received in revised form 12 December 2024; Accepted 15 December 2024
Available online 24 December 2024

List of Abbreviations

AOP	Argument of perigee
CLFD	Closed-loop feedback-driven
CSI	Constant Specific Impulse
Ecc	Eccentricity
GVEs	Gauss Variational Equations
IDs	Integer identifiers
ILP	Integer Linear Programming
Inc	Inclination
LEO	Low Earth Orbit
MEO	Medium Earth Orbit
MILP	Mixed Integer Linear Programming
MTTSP	Moving-Target Traveling Salesman Problem
OSAM	On-orbit Servicing Assembly and Manufacturing
RAAN	Right Ascension of the Ascending Node
RTN	Radial, tangential and out-of-plane frame
SMA	Semi-major axis
STSP	Static Traveling Salesman Problem

J_2 secular effects and the minimum-fuel case is also considered through empirical formulas. The optimal-sequence trajectory is then obtained through indirect optimization methods. Ref. [10] solves the multiple-visitation optimal tour problem for a very large dataset of asteroids. However, a distance metric which neglects the fuel mass depletion is used, that can be applied only in cases of small differences in the orbital elements. A bi-objective MTTSP for a five-debris-object removal mission is solved in Ref. [11]. Their model uses averaged dynamical equations and neglects the phasing maneuver cost. The distance metric accounts for three-element targeting and is evaluated by functions derived by interpolation of pre-computed results. The optimal sequence is found by an exhaustive search algorithm. In Ref. [12], the authors establish a surrogate low-thrust transfer model accounting for secular J_2 and drag perturbations. The computational burden is reduced by adopting an averaged analytical solution of the perturbed Keplerian motion. The combinatorial problem is finally solved by means of heuristics. In Ref. [13], the authors present a solution to remove eight debris objects located in circular geostationary Earth orbits by means of multiple hybrid-propulsion servicing spacecraft. The scheduling optimization problem is solved by means of heuristics. The cost of each orbit-to-orbit maneuver is quantified by adopting a multi-phase strategy. In Ref. [15], the authors solve the optimal multi-target rendezvous problem, combining high-thrust and low-thrust trajectories via an extended minimum-time Q-law [16]. Maneuver costs for single-target rendezvous are calculated at various departure times and incorporated into an Integer Linear Programming (ILP) model to address the combinatorial aspect. However, this framework is applied to a time-dependent formulation, leading to a high number of optimization variables and limiting the approach's scalability. The approach is demonstrated on an open tour problem involving eight satellites in nearly circular Low Earth Orbits (LEO).

In this paper, two different distance metrics – an analytical cost function based on Edelbaum's theory and a Q-law based function – are combined with Mixed Integer Linear Programming (MILP) to find the global optimal visiting sequence of a multi-client servicing mission. The algorithm is composed of two steps. First, the distance metric is employed to evaluate the cost of all possible client-to-client trajectories. Then, the pre-computed results are used in combination with an MILP algorithm to find the sequence such that all the clients are visited once and only once and servicer fuel mass consumption is minimized. One of the key aspects is that no particular assumptions regarding the orbits are needed. In particular, the Q-law is adapted to be used in conjunction with MILP for both minimum-time and minimum-fuel scenarios, providing near-optimal cost estimates for five-orbital-element targeting. The performance in terms of computation time and accuracy of the proposed approach is demonstrated on two datasets of satellites located in Medium Earth Orbit (MEO), consisting of 31 and 42 satellites, respectively.

The main contribution of this paper is the introduction of a new algorithm, MILP/ΔV, which combines a MILP formulation with optimized costs to develop a scalable approach for efficiently computing optimal trajectories in low-thrust multi-client servicing missions, accommodating clients' orbits of any kind, including elliptical ones.

The article is organized as follows. Section 2 reports the problem statement. Section 3 presents the distance metrics adopted. Section 4 presents the algorithm to solve the combinatorial problem. The proposed solution is presented in Section 5. Section 6 shows the numerical results. In Section 7 the conclusions are drawn.

2. Problem formulation

2.1. Assumptions

The MTTSP is difficult to solve because it is time-dependent [17]. In this paper, the following assumptions are made to reduce the MTTSP to a Static TSP (STSP).

Assumption 1 (*Distance Metric*)**.** The cost to transfer between a given ordered pair of satellites depends only on their initial states. This assumption implies that a distance metric form can be defined a priori for each possible transfer. This is a standard assumption when dealing with multiple-visitation problems [4,8,15,17].

Assumption 2 (*Perturbations*)**.** Perturbations are neglected. All satellites are subjected only to Keplerian dynamics.

Assumption 3 (*Rendezvous Cost*)**.** Phasing cost is neglected, i.e., at most five orbital elements are targeted. Ref. [18] demonstrated that the cost difference between a transfer maneuver and a rendezvous maneuver is generally negligible in case of low-thrust propulsion. In particular, the solution of the combinatorial problem is not affected by the fast variable targeting. This is a standard assumption when dealing with multiple-visitation low-thrust problems [8,9,11,12].

One of the possible criteria to determine an optimal sequence is the minimization of the fuel consumption used to visit all of the clients. Assuming no gravitational losses, fuel consumption can be obtained from the transfer cost quantified in terms of ΔV through the Tsiolkovsky equation

$$\Delta m = m_0 \left(1 - e^{-\frac{\Delta V}{g_0 I_{sp}}}\right)$$

where m_0 is the fuel of the satellite before the maneuver, $g_0 = 9.80665\ \mathrm{m/s^2}$ is the gravity at Earth surface, and I_{sp} is the specific impulse of the propulsion system. With this assumption, minimizing ΔV is equal to minimizing the fuel consumption. In Keplerian dynamics (i.e., orbits to visit are fixed in the inertial space), if phasing cost is neglected, the minimum ΔV of each possible leg does not depend on time but only on the characteristics (five classical orbital elements, other than anomaly) of initial and final orbits. Both the mass depletion and time of flight can be then computed from the characteristics of the propulsion system and do not influence the selection of the next client to visit.

The assumptions outlined above offer the following key advantages:

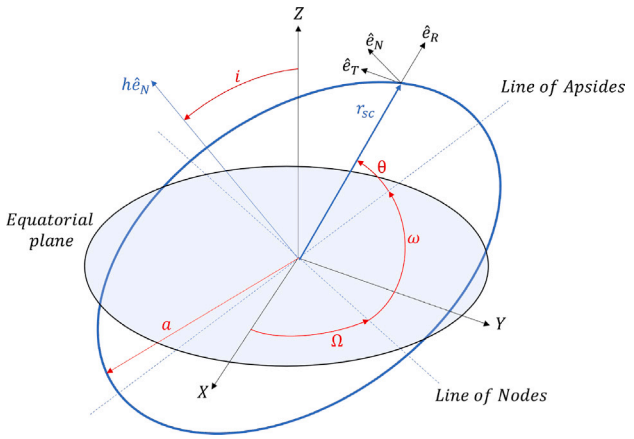

Fig. 1. Diagram of the RTN frame, indicated by the unit vectors $\hat{e}_R$, $\hat{e}_T$, and $\hat{e}_N$.

- The transfer cost between any ordered pair of satellites (i, j) is independent of time and symmetric with respect to index permutation.
- The problem can be formulated as a MILP problem, ensuring convergence to the global optimum.

These considerations allow the problem to be formulated in a minimal form, reducing the number of optimization variables to its lowest possible level, thereby enhancing the scalability of the proposed approach. The impact of Assumptions 2 and 3 on the solutions will be assessed in Section 6.2.1.

2.2. Dynamic model

Let $\mathbf{X}_S(t) = [a(t), e(t), i(t), \Omega(t), \omega(t), \theta(t), m(t)]_S^{\mathsf{T}}$ be the state of the servicer, where $a(t)$ is the semi-major axis (SMA), $e(t)$ the eccentricity (Ecc), $i(t)$ the inclination (Inc), $\omega(t)$ the argument of perigee (AOP), $\Omega(t)$ the RAAN, $\theta(t)$ the true anomaly, and $m(t)$ is the mass. Let $\mathbf{T}(t)$ be the control thrust described in the radial, transverse and out-of-plane (RTN) frame (see Fig. 1 for a visual representation). The dynamics of the servicer can be therefore written by using the Gauss Variational Equations (GVEs) [19] as

$$\dot{\mathbf{X}}_S(t) = \mathcal{F}(\mathbf{X}_S(t), \mathbf{T}(t)) = \begin{bmatrix} \boldsymbol{A}\frac{\mathbf{T}}{m} \\ -\frac{\|\mathbf{T}\|}{g_0 I_{sp}} \end{bmatrix} + \begin{bmatrix} \mathbf{b} \\ 0 \end{bmatrix} \tag{1}$$

where $\mathbf{A} \in \mathbb{R}^{6\times 3}$ and $\mathbf{b} \in \mathbb{R}^{6\times 1}$. Denoting with $p = a(1-e^2)$ the semi-latus rectum, with $h = \sqrt{\mu p}$ the angular momentum and with $r_{SC} = p/(1 + e\cos\theta)$ the distance of the satellite with respect to the center of the Earth, the following equations hold

$$\mathbf{A} = \begin{bmatrix} \frac{p\cos(\theta)}{he} & \boldsymbol{B} & \frac{-(p+r_{SC})\sin(\theta)}{he} & 0 \end{bmatrix} \tag{2}$$

$$\boldsymbol{B} = \begin{bmatrix} \frac{2a^2 e\sin(\theta)}{h} & \frac{2a^2}{h}\frac{p}{r_{SC}} & 0 \\ \frac{p\sin(\theta)}{h} & \frac{(p+r_{SC})\cos(\theta)+r_{SC}e}{h} & 0 \\ 0 & 0 & \frac{r_{SC}\cos(\omega+\theta)}{h} \\ 0 & 0 & \frac{r_{SC}\sin(\omega+\theta)}{h\sin(i)} \\ -\frac{p\cos(\theta)}{he} & \frac{(p+r_{SC})\sin(\theta)}{he} & -\frac{r_{SC}\sin(\omega+\theta)}{h\tan(i)} \end{bmatrix} \tag{3}$$

$$\mathbf{b} = \begin{bmatrix} \mathbf{0}_{5\times 1} \\ \frac{h}{r_{SC}^2} \end{bmatrix} \tag{4}$$

where $\mu = 3.986 \times 10^{14}$ m^3/s^2 is the gravitational constant of the Earth. Eq. (3) represents the GVEs for the slow variables. Finally, let $\mathbf{X}_i(t) = [a, e, i, \Omega, \omega, \theta(t), m(t)]_i^{\mathsf{T}}$ be the state of the ith client. Assuming uncontrolled motion, the following holds

$$\dot{\mathbf{X}}_i(t) = \mathcal{F}(\mathbf{X}_i(t), \mathbf{0}) = \mathcal{G}_i(\mathbf{X}_i(t)). \tag{5}$$

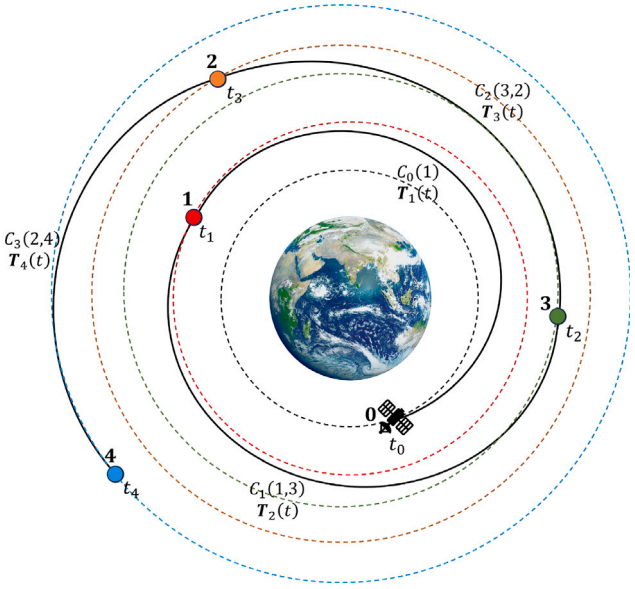

Fig. 2. Schematic representation of servicer trajectory for a multiple-visitation mission.

2.3. Static TSP problem statement

The STSP represents the archetype of multiple-visitation problems where a salesman has to visit all cities of a dataset once and only once. Let $\mathcal{K} = \{1, 2, \ldots, i, \ldots, N_{sat}\}$ be the set of integer identifiers (IDs) associated with N_{sat} clients to be serviced. A visiting sequence is defined by an ordered set $\mathcal{D} = \{d_1, \ldots, d_i, \ldots, d_{N_{sat}}\}$ where $d_i \in \mathcal{K}, \forall i \in \mathcal{K}$. A set of N_{sat} functions $\mathcal{T} = \{\mathbf{T}_1(t), \ldots, \mathbf{T}_i(t), \ldots, \mathbf{T}_{N_{sat}}(t)\}$ is used to denote the servicer control law to perform the ith visitation.

Let $C_0(d_1)$ represent the cost of going from the initial servicer orbit to satellite d_1, and let $C_i(d_i, d_{i+1}), \forall i \in \{1, \ldots, N_{sat}-1\}$ be the cost of going from satellite d_i to satellite d_{i+1}. Then, the total cost J to be minimized can be written as

$$J(\mathcal{D}) = C_0(d_1) + \sum_{i=1}^{N_{sat}-1} C_i(d_i, d_{i+1}). \tag{6}$$

Example: Let $N_{sat} = 4$ represent the number of clients to be visited, and define the sequence of target orbits as $\mathcal{D} = \{d_1, d_2, d_3, d_4\} = \{1, 3, 2, 4\}$. Consider a servicer initially located in orbit 0 at time t_0. The set of servicer control laws is given by $\mathcal{T} = \{\mathbf{T}_1(t), \mathbf{T}_2(t), \mathbf{T}_3(t), \mathbf{T}_4(t)\}$, and let t_i, for $i \in \{1, 2, 3, 4\}$, represent the time at which the servicer reaches the client orbit d_i. Fig. 2 illustrates the complete servicer trajectory for this case. Note that each transfer actually includes many revolutions with low-thrust, but they are not shown in Fig. 2 for clarity.

In this case, the total cost associated with the sequence $\mathcal{D}$ is

$$J(\mathcal{D}) = C_0(1) + C_1(1,3) + C_2(3,2) + C_3(2,4).$$

The STSP can be stated as follows

STSP Problem Statement

$$\min_{\mathcal{D}} J(\mathcal{D}) = \min_{\mathcal{D}} \left(C_0(d_1) + \sum_{i=1}^{N_{sat}-1} C_i(d_i, d_{i+1}) \right)$$

subject to

$$\begin{aligned}
&\dot{\mathbf{X}}_S(t) = \mathcal{F}\left(\mathbf{X}_S(t), \mathbf{T}_i(t)\right) && \forall t, \forall i \in \mathcal{K} \\
&\|\mathbf{T}_i(t)\| \leq T_{max} && \forall t, \forall i \in \mathcal{K} \\
&\dot{\mathbf{X}}_i(t) = \mathcal{G}_i\left(\mathbf{X}_i(t)\right) && \forall t, \forall i \in \mathcal{K} \\
&\mathbf{X}_S(t_0) = \mathbf{X}_{S,0} && \\
&\mathbf{X}_i(t_0) = \mathbf{X}_{i,0} && \forall i \in \mathcal{K} \\
&\underline{\mathbf{X}_{S,[1:5]}(t_i) = \mathbf{X}_{d_i,[1:5]}} && \forall i \in \mathcal{K} \\
&\mathcal{D} = \left\{ d_1, ..., d_{N_{sat}} \right\} && \\
&d_i \in \mathcal{K} && \forall i \in \mathcal{K} \\
&d_i \neq d_j && \forall i, j \in \mathcal{K}, i \neq j
\end{aligned}$$

where T_{max} is the maximum available thrust, $\mathbf{X}_S(t_0)$ represents the state of the servicer at initial time t_0, while $\mathbf{X}_i(t_0)$ that of the ith client. The constraint $\underline{\mathbf{X}_{S,[1:5]}(t_i) = \mathbf{X}_{d_i,[1:5]}}$ underlines that the first five orbital elements (subscript $[1:5]$) of the servicer and client d_i have to be the same at time t_i.

Since perturbations are neglected and angular position is not targeted, equation $\mathbf{X}_{S,[1:5]}(t_i) = \mathbf{X}_{d_i,[1:5]}$ represents the boundary condition of a five orbital element transfer maneuver.

The considerations in Section 2.1 allow the leg cost functional to be solved a priori, yielding both $\mathbf{T}_i(t)$ and t_i for each transfer in a given sequence. This approach defines a cost function J that depends solely on the sequence, thereby reducing the MTTSP to a combinatorial optimization problem.

The problem now consists of finding the sequence that minimizes J. The following sections present the distance metrics adopted and the algorithm used to solve the STSP.

3. Orbit distance metrics

3.1. Improved edelbaum distance metric

Edelbaum's pioneering work [20] reports the ΔV required to transfer a satellite between two circular orbits which differ only in inclination and semi-major axis. The result is obtained by averaging the GVEs (Eq. (1)), and considering constant control acceleration. This distance metric results are accurate when orbits with the same RAAN are considered. As documented in Ref. [20], inclination and RAAN change maneuvers are the most expensive; thus, it is essential to have a distance metric which accounts for RAAN correction. Ref. [21] improved Edelbaum's solution in order to account for the RAAN targeting. The solution is found in terms of ΔV in the minimum-time context adopting similar assumptions made in Ref. [20] and splitting the transfer into two phases, the first correcting the velocity difference (which, for circular orbits, is equivalent to semi-major axis correction) and the inclination (V, i) and the second correcting the velocity and the RAAN (V, Ω). Ref. [21] also presented an alternative strategy where the two phases are performed in reverse order (i.e., (V, Ω) and (V, i)). Ref. [22] combines the two strategies to find a $\Delta V_{Ed,\Omega}$ expression accounting for simultaneous correction of velocity, inclination and RAAN (V, i, Ω), written as

$$\begin{aligned}
\Delta V_{Ed,\Omega}(d_i, d_j) &= \sqrt{V_{d_i}^2 + V_{d_j}^2 - 2V_{d_i}V_{d_j}\cos\left(\frac{\pi}{2}g\right)} \\
g(i_{d_i}, i_{d_j}, \Omega_{d_i}, \Omega_{d_i}) &= \sqrt{\Delta i^2 + \sin^2(\bar{i})\Delta\Omega^2}
\end{aligned} \tag{7}$$

where d_i and d_j indicate the IDs of the initial and final orbits, $V_{d_i} = \sqrt{\mu/a_{d_i}}$ and $V_{d_j} = \sqrt{\mu/a_{d_j}}$ are their orbital velocity magnitudes of the corresponding circular orbits, $\Delta i = i_{d_j} - i_{d_i}$, $\Delta\Omega = \Omega_{d_j} - \Omega_{d_i}$ and $\bar{i} = \left(i_{d_j} + i_{d_i}\right)/2$ is the mean inclination. Eq. (7) accounts only for three orbital elements targeting (a, i, Ω) in minimum-time framework and neglects the fuel mass depletion during the transfer. In addition, its symmetric nature ($\Delta V_{Ed,\Omega}(d_i, d_j) = \Delta V_{Ed,\Omega}(d_j, d_i)$) makes it suitable for the MILP algorithm presented in the next sections.

3.2. Q-law based distance metric

3.2.1. Q-law overview

Q-law is a closed-loop feedback-driven (CLFD) guidance method first proposed by Petropoulos [23] and based on Lyapunov's second theorem [24].

Let $\overline{\mathbf{X}}(t) = [a(t), e(t), i(t), \Omega(t), \omega(t)]^\intercal$ be the state of the spacecraft represented by the Keplerian elements (neglecting the fast variable θ), let $\mathbf{X}_T = [a_T, e_T, i_T, \Omega_T, \omega_T]^\intercal$ be a fixed target state, let $\mathbf{Z} = \overline{\mathbf{X}}(t) - \mathbf{X}_T$ be the error state, by using Eqs. (1) and (3) the following holds

$$\dot{\mathbf{Z}} = \frac{\partial \mathbf{Z}}{\partial t} = \dot{\overline{\mathbf{X}}}(t) - \dot{\mathbf{X}}_T = \dot{\overline{\mathbf{X}}}(t) = \mathbf{B}\mathbf{u}(t) \tag{8}$$

where $\mathbf{u}(t) = \mathbf{T}(t)/m(t)$ is the vector of control acceleration. In this case, it is possible to write the time derivative of the general Lyapunov function $Q(\mathbf{Z})$ as

$$\dot{Q}(\mathbf{Z}) = \frac{\partial Q(\mathbf{Z})}{\partial t} = \frac{\partial Q(\mathbf{Z})}{\partial \mathbf{Z}}\frac{\partial \mathbf{Z}}{\partial t} = \frac{\partial Q(\mathbf{Z})}{\partial \mathbf{Z}}\mathbf{B}\mathbf{u}. \tag{9}$$

For a given Lyapunov function, it is possible to obtain near-optimal minimum-time trajectories by minimizing its time derivative at each instant by choosing

$$\mathbf{u} = -\mathbf{B}^T \frac{\partial Q(\mathbf{Z})}{\partial \mathbf{Z}}^T. \tag{10}$$

Ref. [23] proposes the following Lyapunov function

$$Q(\mathbf{Z}) = \left(1 + W_P P\right) \sum_{i=1}^{5} W_i S_i \left(\frac{\delta Z_i}{\max_\theta(\dot{X}_i)} \right)^2 \tag{11}$$

$$\delta\mathbf{Z} = \begin{bmatrix} a - a_T \\ e - e_T \\ i - i_T \\ \arccos\left(\cos\left(\Omega - \Omega_T\right)\right) \\ \arccos\left(\cos\left(\omega - \omega_T\right)\right) \end{bmatrix} \tag{12}$$

where $W_P \geq 0, W_i \geq 0$ are user-defined parameters and could be adjusted in order to prioritize the convergence of a specific orbital element. P and S_i are predefined functions and $\max_\theta(\dot{X}_i)$ is the maximum rate of change of the orbital element X_i with respect to true anomaly over the current osculating orbit and can be calculated analytically for all elements except ω, in case of Keplerian dynamics. The analytic expressions of these terms and further details can be found in Ref. [23]. From Eqs. (11) and (12) it is possible to compute the analytic expression of $\partial Q(\mathbf{Z})/\partial \mathbf{Z}$ and from Eq. (10) the control acceleration at each instant by using the osculating orbital elements. It is sufficient to integrate the system starting with initial orbital elements using the control in Eq. (10) in order to drive the satellite to the target; the integration is stopped when $\|\delta Z_i\| \leq \epsilon_i$, $\forall i = \{1, \ldots, 5\}$ where ϵ_i is the ith orbital element predefined tolerance.

In the case where the propulsion system has a limited maximum thrust, it is possible to modify Eq. (10) as

$$\begin{aligned}
\mathbf{u} &= \frac{T_{max}}{m}\left(\frac{-\mathbf{B}^T \frac{\partial Q(\mathbf{Z})}{\partial \mathbf{Z}}^T}{\|\mathbf{B}^T \frac{\partial Q(\mathbf{Z})}{\partial \mathbf{Z}}^T\|} \right) \\
&= \frac{T_{max}}{m}\begin{bmatrix} \sin(\alpha)\cos(\beta) \\ \cos(\alpha)\cos(\beta) \\ \sin(\beta) \end{bmatrix} = \frac{T_{max}}{m}\hat{\mathbf{u}}
\end{aligned} \tag{13}$$

where α and β denote the in-plane and out-of-plane angles of the thrust, respectively (see Fig. 3 for a visual representation).

When the minimization of the fuel is the objective of the optimization problem, the optimal control solution is composed of maximum-thrust-arcs and thrust-off-arcs (coast arcs) [25,26]. Previous derivation

of the Q-law did not consider a mechanism to switch the thrust off. A switch-off strategy is presented in Ref. [27] where two additional parameters, the so-called relative and absolute effectivities (η_r and η_a), are defined. These parameters introduce coast arcs at points where the engine thrust is less efficient and they are defined as

$$\begin{aligned} \eta_a &= \frac{\min_{\alpha,\beta}(\dot{Q})}{\min_\theta\left(\min_{\alpha,\beta}(\dot{Q})\right)} \\ \eta_r &= \frac{\min_{\alpha,\beta}(\dot{Q}) - \max_\theta\left(\min_{\alpha,\beta}(\dot{Q})\right)}{\min_\theta\left(\min_{\alpha,\beta}(\dot{Q})\right) - \max_\theta\left(\min_{\alpha,\beta}(\dot{Q})\right)} \end{aligned} \tag{14}$$

where $\min_{\alpha,\beta}(\dot{Q})$ is the minimum of the time derivative of the Lyapunov function with respect to α and β evaluated at the osculating orbital elements (including anomaly) and are computed by using Eq. (10) as

$$\min_{\alpha,\beta}(\dot{Q}) = \min_{\alpha,\beta}\left(\left(\frac{\partial Q}{\partial \boldsymbol{Z}}\right)\boldsymbol{B}\boldsymbol{u}\right) = -\left\|\boldsymbol{B}^T\left(\frac{\partial Q}{\partial \boldsymbol{Z}}\right)^T\right\|$$

while $\min_\theta\left(\min_{\alpha,\beta}(\dot{Q})\right)$ and $\max_\theta\left(\min_{\alpha,\beta}(\dot{Q})\right)$ are respectively the minimum and the maximum of the time derivative of the Lyapunov function with respect to α, β and θ over an entire orbit ($\theta \in [0, 2\pi]$); these quantities cannot be expressed in closed form and they have to be obtained numerically (for example through a grid search algorithm). The parameters η_r and η_a attempt to quantify the effectiveness in changing the orbital parameters at a given osculating point compared to the optimum point for changing the orbital parameters over a complete orbit. When certain thresholds are set ($\overline{\eta}_r$, $\overline{\eta}_a$), the control law derived using Q-law has the following form

$$\mathbf{u} = \begin{cases} \mathbf{0}, & if \quad \eta_r \le \overline{\eta}_r \ or \ \eta_a \le \overline{\eta}_a \\ \frac{T_{max}}{m}\begin{bmatrix} \sin(\alpha)\cos(\beta) \\ \cos(\alpha)\cos(\beta) \\ \sin(\beta) \end{bmatrix}, & otherwise. \end{cases} \tag{15}$$

As in the minimum-time case, the time of flight of the transfer is a consequence of selected parameters and stopping criteria.

The control laws given in Eqs. (13) and (15) mimic the results obtained by applying Pontryagin's Minimum Principle respectively to the minimum-time and minimum-fuel space trajectories [25] in the case of a Constant Specific Impulse (CSI) propulsion system (i.e., the optimal trajectory is composed of maximum-thrust-always-on arcs in the minimum-time formulation and maximum-thrust-arcs and thrust-off-arcs in the minimum-fuel formulation).

The Q-law can be generalized to include main perturbations (secular J_2, drag, eclipse) maintaining the same form for the control acceleration (i.e., perturbations are not included into $\mathbf{B}$) but using the osculating orbital elements obtained by the propagation of the perturbed dynamics [28]. Q-law has been also reformulated for equinoctial elements [29] or for six elements targeting [8,30].

3.2.2. Derivation of Q-law based distance metric

Once the servicer initial mass m_0 and the characteristics of its propulsion system are defined (T_{max}, I_{sp}), Q-law computes the mass history $m(t)$ and the final transfer time t_f. Fuel mass depletion can be computed as $\Delta m = m_0 - m(t_f)$ and represents a possible distance metric. However, in multiple-visitation problems, the initial mass strictly depends on the previously visited satellites (i.e., the sequence and the costs are no longer independent). Employing such a distance metric would require the evaluation of all possible sequences. A different approach to bypass this sequence dependency is proposed in this article. It consists of using Q-law cost estimation in terms of ΔV which, in Keplerian dynamics, only depends on initial and final orbital elements and strategy (minimum-time or minimum-fuel). For a generic transfer from orbit d_i to orbit d_j, Q-law can provide the mass of the servicer as a function of time $m_{d_i\to d_j}(t)$ and the so-called switching function $B_{d_i\to d_j}(t)$ ($B_{d_i\to d_j}(t) = 1$ if the thrust is on at instant t, while $B_{d_i\to d_j}(t) = 0$ otherwise). From mass and switching histories, it is possible to compute

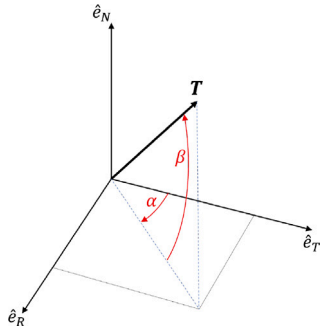

Fig. 3. Illustration of the in-plane angle α and out-of-plane angle β of the thrust.

the increment in velocity $\Delta V_{QL}(d_i, d_j)$ and the duty cycle $DC_{QL}(d_i, d_j)$ through the following integrals

$$\Delta V_{QL}(d_i, d_j) = \int_{t_{0,d_i}}^{t_{f,d_i\to d_j}} \frac{T_{max}}{m_{d_i\to d_j}(t)} B_{d_i\to d_j}(t)dt \tag{16}$$

$$DC_{QL}(d_i, d_j) = \frac{1}{t_{f,d_i\to d_{i+1}}} \int_{t_{0,d_i}}^{t_{f,d_i\to d_j}} B_{d_i\to d_j}(t)dt \tag{17}$$

where t_{0,d_i} is the initial transfer time when servicer departs from orbit d_i while $t_{f,d_i\to d_j}$ is the time of flight returned by the convergence of the Q-law. It is evident that in the minimum-time case, $DC_{d_i\to d_j} = 1$ since $B_{d_i\to d_j}(t) = 1, \forall t \in \left[t_{0,d_i}, t_{f,d_i\to d_j}\right]$, while in the minimum-fuel case, the duty cycle depends on relative and absolute effectivity thresholds ($\overline{\eta}_r$ and $\overline{\eta}_a$). Considering the assumptions presented in previous sections, it is also true that $\Delta V_{QL}(d_i, d_j) = \Delta V_{QL}(d_j, d_i)$ and $DC_{QL}(d_i, d_j) = DC_{QL}(d_j, d_i)$.

4. Combinatorial problem

In this section, the MILP problem formulation is presented in detail. We use the term *leg* to define the generic transfer between two orbits and the functions $\Delta V_{Ed,\Omega}$ and ΔV_{QL} to represent the distance metrics that quantify the cost of each leg in terms of ΔV. The ultimate goal is to find the sequence of satellites to visit which minimizes the total cost.

MILP [31] is a computationally efficient method to find the solution of problems involving linear cost and linear constraints. The optimization variables can be either continuous or integer variables. In case of integer optimization variables, the problem solved by MILP solvers can be stated as follows

MILP Problem Definition

$$\min_{\mathbf{y}} \ \mathbf{w}^T\mathbf{y}$$

subject to

$$\begin{aligned} &\mathbf{y} \in \mathbb{N}^m \\ &\mathbf{y}_{lb} \le \mathbf{y} \le \mathbf{y}_{ub} \\ &\mathbf{A}_{eq}\mathbf{y} = \mathbf{b}_{eq} \\ &\mathbf{A}_{ineq}\mathbf{y} \le \mathbf{b}_{ineq} \end{aligned}$$

where $\mathbf{y} = [y_1, \dots, y_m]^\intercal$ is the vector of optimization variables, $\mathbf{w} \in \mathbb{R}^m$ is the vector containing the cost associated with each optimization variable, $\mathbf{y}_{lb}$ and $\mathbf{y}_{ub}$ are the boundary constraints of the optimization variables, $\mathbf{A}_{eq} \in \mathbb{R}^{l\times m}$ and $\mathbf{b}_{eq} \in R^l$ are the equality constraints matrix and vector, respectively, $\mathbf{A}_{ineq} \in \mathbb{R}^{p\times m}$ and $\mathbf{b}_{ineq} \in \mathbb{R}^p$ represent the inequality constraints matrix and vector.

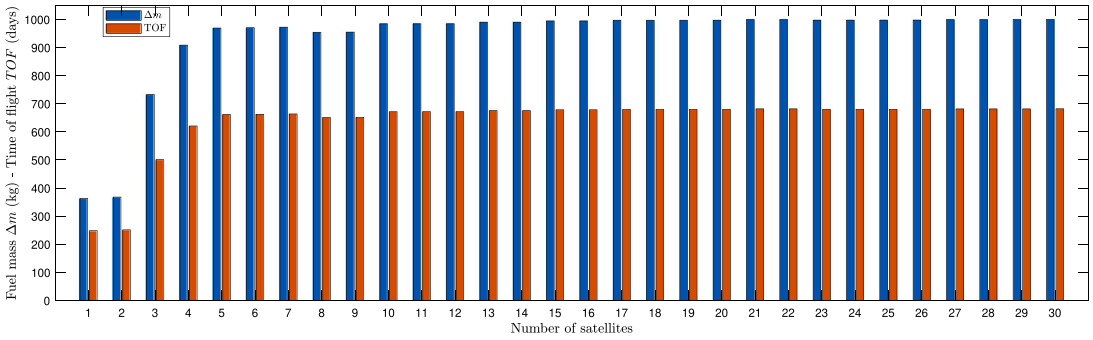

Fig. 4. Fuel mass depletion and time of flight for an increasing number of satellites.

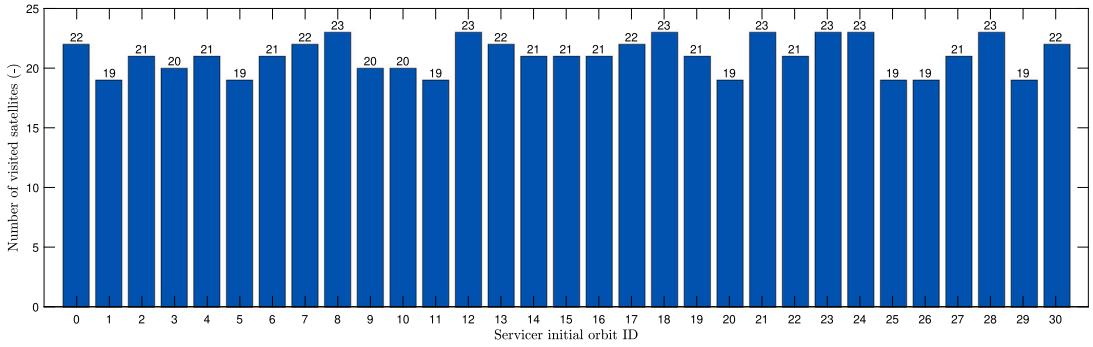

(a) Number of visited clients.

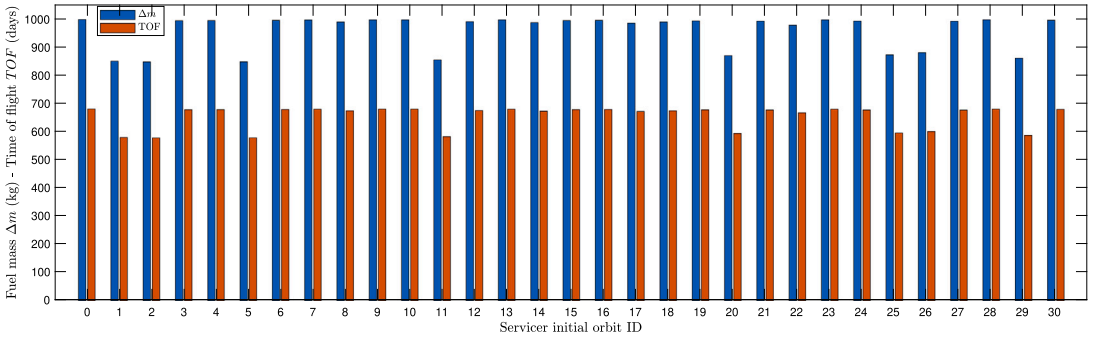

(b) Fuel mass depletion and time of flight.

Fig. 5. Servicer initial orbit analysis.

Based on the STSP definition, it is possible to consider the following optimization variable $\mathbf{y} \in \mathbb{B}^m$ and cost vector $\mathbf{w} \in \mathbb{R}_+^m$

$$\mathbf{y} = \begin{bmatrix} y_{0\to 1} \\ \vdots \\ y_{0\to N_{sat}} \\ y_{1\to 2} \\ \vdots \\ y_{1\to N_{sat}} \\ \vdots \\ y_{N_{sat}-1\to N_{sat}} \end{bmatrix} \quad \mathbf{w} = \begin{bmatrix} w_{0\to 1} \\ \vdots \\ w_{0\to N_{sat}} \\ w_{1\to 2} \\ \vdots \\ w_{1\to N_{sat}} \\ \vdots \\ w_{N_{sat}-1\to N_{sat}} \end{bmatrix} \tag{18}$$

where the subscripts $0, 1, \ldots, N_{sat}$ denote the IDs of the orbits, 0 is the ID related to the initial servicer orbit, while the general component of the optimization vector $y_{i\to j} \in \{0, 1\}$ takes the value of 1 if the transfer from ith orbit to jth is performed (i.e., selection of the $i \to j$ leg) and 0 otherwise. $w_{i\to j} \in \mathbb{R}_+$ represents the cost associated with the transfer from ith to jth orbit. Note that this definition assumes symmetric costs (i.e., $w_{i\to j} = w_{j\to i}$). This assumption is automatically satisfied when the time and sequence dependencies are neglected and the ΔV is used as distance metric. Given that the number of possible departure orbits equals $N_{sat}+1$, and the number of possible final orbits equals N_{sat}, and considering symmetric costs, the number of distance metric evaluations is

$$m = \frac{(N_{sat}+1)N_{sat}}{2}. \tag{19}$$

Eq. (19) represents the computational complexity of the proposed approach, regardless of the chosen distance metric. It quantifies the number of transfer cost evaluations required to solve the combinatorial problem, drastically reducing the computational burden compared to an exhaustive search algorithm where the sequences to evaluate are on the order of $N_{sat}!$. This minimal complexity formulation further reduces computational cost compared to existing methods [8,12,15], allowing its application to larger satellite datasets.

Eq. (18) allows for a graph representation of the problem where the nodes of the graph represent all of the orbits of the dataset and the edges connecting them represent the selected transfer maneuvers. The graph visualization makes it easier to derive the set of equality and inequality constraints. Recalling that the problem consists of visiting

all of the clients once starting from a given initial orbit, and that $\mathbf{y}$ is a vector of booleans, the constraints can be expressed as follows

$$\mathbf{y}_{lb} = \mathbf{0}_{m\times 1} \tag{20a}$$

$$\mathbf{y}_{ub} = \mathbf{1}_{m\times 1} \tag{20b}$$

$$\sum_{j=1}^{N_{sat}} y_{0\to j} = 1 \tag{20c}$$

$$\sum_{j=1}^{m} y_j = N_{sat} - 1 \tag{20d}$$

$$1 \le \sum_{j=0}^{i-1} y_{j\to i} + \sum_{j=i+1}^{N_{sat}} y_{i\to j} \le 2 \quad \forall i = \{1,\dots,N_{sat}\}. \tag{20e}$$

Eqs. (20a) and (20b) imply that the solution has to be composed of booleans, Eq. (20c) requires that the node relative to the initial servicer orbit can have only one edge, Eq. (20d) assures that the number of edges equals $N_{sat} - 1$. Eqs. (20e) guarantee that, except for the node relative to the initial servicer orbit, each node can be connected to the others at least once and maximum twice (once if the node is the final orbit, twice if it is an intermediate orbit). Eqs. (20) can be easily converted into matrix form and furnished to the MILP solver. It is important to underline that Eqs. (20) are not sufficient to find an open tour where all of the nodes are connected constituting a continuous sequence. In fact, a solution where clusters of nodes are linked in a closed form can satisfy the constraints without representing a visitation sequence (presence of subtours). For instance, if we consider five nodes, with the initial servicer location denoted by index 0, a solution where node 0 is connected to one of the nodes while the remaining ones are linked together satisfies Eqs. (20), but it does not represent a visiting sequence. To solve this problem, the solution given by the MILP solver must be checked iteratively by excluding the subtours until a feasible solution is found. An efficient strategy consists in introducing inequality constraints, one per subtour, in order to exclude all possible re-combinations of the nodes of the subtour in the following iteration. Denoting with $\mathbf{y}^i_{opt}$ the optimal solution for the ith iteration, the algorithm for the derivation of such inequalities is outlined in Algorithm 1. Finally, the MILP based algorithm to solve the STSP can be written as in Algorithm 2.

Algorithm 1 Subtours Inequality Constraints

1: Given the i^{th} iteration solution $\mathbf{y}^i_{opt}$
2: $N_{ST} \leftarrow$ Number of subtours in $\mathbf{y}^i_{opt}$
3: $j \leftarrow 1$
4: **while** $j \le N_{ST}$ **do**
5: $\quad \mathbf{M} \leftarrow$ Indices of $\mathbf{y}^i_{opt}$ components constituting the subtour
6: $\quad N_{edges} \leftarrow$ Number of the subtour edges
7: $\quad$ Add $\sum_{z\in\mathbf{M}} y_z \le N_{edges} - 1$ to constraints
8: $\quad j \leftarrow j + 1$
9: **end while**

5. Proposed solution

The Q-law based distance metric is capable of obtaining near-optimal ΔV and time of flight for both minimum-time and minimum-fuel cases. Although Q-law cost computation is relatively fast, its application within the exhaustive algorithm could result in prohibitive computational time when a large dataset is considered. The distance metric in Eq. (16) has been coupled with MILP to derive a new algorithm (MILP/ΔV_{QL}) that overcomes these computational bottlenecks while guaranteeing an accurate estimation in terms of ΔV for five-element orbit transfer. By exploiting the symmetry of the ΔV_{QL} distance metric, it is possible to compute and store the weights needed by MILP

Algorithm 2 MILP based STSP

1: Define N_{sat}
2: Choose leg cost function $J = J(y_{i\to j})$
3: Compute $\mathbf{w} = \left[J(y_{0\to 1}),\dots,J(y_{N_{sat}-1\to N_{sat}})\right]^T$
4: Write constraints (Eqs. (20))
5: $\mathbf{y}^1_{opt} \leftarrow$ MILP solver first solution
6: Compute number of subtours $N_{ST}\left(\mathbf{y}^1_{opt}\right)$
7: **while** $N_{ST} > 1$ **do**
8: $\quad$ Add constraints to exclude subtours (Algorithm 1)
9: $\quad \mathbf{y}^i_{opt} \leftarrow$ MILP solver i^{th} solution
10: $\quad$ Compute number of subtours $N_{ST}\left(\mathbf{y}^i_{opt}\right)$
11: **end while**

algorithm in the $\mathbf{w}_{QL}$ vector and the associated duty cycles in the $\mathbf{DC}_{QL}$ vector by Eqs. (16) and (17)

$$\mathbf{w}_{QL} = \begin{bmatrix} \Delta V_{QL}(0,1) \\ \vdots \\ \Delta V_{QL}(0,N_{sat}) \\ \Delta V_{QL}(1,2) \\ \vdots \\ \Delta V_{QL}(N_{sat}-1,N_{sat}) \end{bmatrix} \qquad \mathbf{DC}_{QL} = \begin{bmatrix} DC_{QL}(0,1) \\ \vdots \\ DC_{QL}(0,N_{sat}) \\ DC_{QL}(1,2) \\ \vdots \\ DC_{QL}(N_{sat}-1,N_{sat}) \end{bmatrix}. \tag{21}$$

The quantities given in Eq. (21) can be used within MILP framework to initialize the MILP/ΔV_{QL} algorithm (Algorithm 3). Algorithm 3 returns the sequence ($\mathcal{D}_{opt} = \left\{\overline{d}_1,\dots,\overline{d}_i,\dots,\overline{d}_{N_{sat}}\right\}$) which minimizes the total ΔV. Once the optimal sequence has been found, it is possible to extract the associated components from the stored vectors $\mathbf{w}_{QL}$ and $\mathbf{DC}_{QL}$ to obtain the costs and duty cycles associated with the optimal sequence as

Algorithm 3 MILP/ΔV_{QL}

1: Define N_{sat}
2: Define Q-law parameters (W_P,W_i,$\overline{\eta}_r$,$\overline{\eta}_a$,ϵ_i)
3: Choose minimum-time or minimum-fuel
4: Compute and store $\mathbf{w}_{QL}$ and $\mathbf{DC}_{QL}$ vectors (Eq. (21))
5: Find the optimal sequence by using Algorithm 2

$$\mathbf{\Delta V}_{opt}(\mathcal{D}_{opt}) = \begin{bmatrix} \Delta V_{QL}(0,\overline{d}_1) \\ \vdots \\ \Delta V_{QL}(\overline{d}_{N_{sat}-1},\overline{d}_{N_{sat}}) \end{bmatrix} \qquad \mathbf{DC}_{opt}(\mathcal{D}_{opt}) = \begin{bmatrix} DC_{QL}(0,\overline{d}_1) \\ \vdots \\ DC_{QL}(\overline{d}_{N_{sat}-1},\overline{d}_{N_{sat}}) \end{bmatrix}. \tag{22}$$

Eq. (22) can be used to retrieve mass depletion and time of flight of each transfer for a generic servicer satellite with initial mass m_0, maximum available thrust T_{max} and specific impulse of the propulsion system I_{sp}. Total fuel consumption Δm and total time of flight TOF of the entire sequence are easily found by summing up the contributions of

Table 1
Servicer satellite properties.

Parameter	Unit	Value
Initial mass m_0	kg	2000
Propellant mass m_{fuel}	kg	1000
Specific impulse I_{sp}	s	3000
Maximum thrust T_{max}	N	0.5
Maximum velocity change ΔV_{max}	km/s	20.392

each leg. The procedure, based on an iterative procedure which updates the servicer mass during the trajectory, is reported in Algorithm 4.

Algorithm 4 MILP/ΔV_{QL} Δm and TOF computation

$m_1 \leftarrow m_0$
$TOF \leftarrow 0$
$i \leftarrow 1$
while $i \leq N_{sat}$ **do**
  $m_{i+1} \leftarrow m_i \left(e^{-\frac{\Delta V_{opt,i}}{g_0 I_{sp}}} \right)$
  $f_i \leftarrow \frac{T_{max}}{0.5(m_i + m_{i+1})} DC_{opt,i}$
  $TOF \leftarrow TOF + \frac{\Delta V_{opt,i}}{f_i}$
  $i \leftarrow i + 1$
end while
$\Delta m \leftarrow m_0 - m_i$

The quantity f_i represents an estimation of the average acceleration available during the ith transfer. In this form, MILP/ΔV_{QL} accurately maintains the estimated mass depletion and time of flight the Q-law would return if evaluated on the same sequence with a specific servicer satellite. The introduction of Eq. (17) is meant to apply the methodology also in the minimum-fuel context. The computational bottlenecks associated with a large dataset are addressed by reducing the number of Q-law evaluations to only those defined by Eq. (19).

Analogous results hold if the analytical cost function $\Delta V_{Ed,\Omega}$ is employed. In this case, the duty cycle of each maneuver equals 1 and Algorithm 4 can be employed to retrieve the fuel mass consumption and time of flight associated with the optimal sequence.

6. Simulations and results

The distance metrics presented in Section 3 have been applied in combination with MILP to solve the STSP. The algorithms have been tested on two different datasets in order to show their performance on realistic satellite constellations.

Table 1 reports the servicer satellite properties used in the simulations [32]. The fuel mass m_{fuel} was assumed to be 50% of the total mass, and ΔV_{max} is the maximum velocity change that can be achieved using the whole propellant mass. All numerical simulations were performed in MATLAB version R2020b on a laptop with one 11th Gen Intel(R) Core(TM) i7 2.3 GHz processor using a 64-bit Windows operating system and 32 GB of RAM.

6.1. GPS constellation test case

For near-circular orbits, Eq. (7) provides a good estimation of the ΔV transfer cost for a low-thrust propulsion system. MILP has been applied with this analytic cost function on a dataset of 31 satellites taken from the GPS constellation. The same initial Keplerian elements as used in Ref. [33] are adopted and reported in Table 2. The optimal sequence, the total cost in terms of ΔV, fuel mass consumption Δm, total time of flight and the computational time as obtained by the MILP are reported in Table 3 for an increasing number of satellites

Table 2
GPS constellation servicer and clients initial Keplerian elements.

ID	a (km)	e	i (deg)	Ω (deg)	ω (deg)
0	26 560.35	6.46e−03	55.53	150.07	53.200
1	26 560.46	4.78e−03	54.18	72.930	188.43
2	26 561.19	1.37e−02	55.12	146.99	254.56
3	26 561.01	1.28e−02	55.42	267.35	41.450
4	26 560.44	2.47e−02	55.07	17.500	309.60
5	26 560.92	8.85e−03	55.91	328.36	127.48
6	26 572.91	2.04e−02	55.39	17.680	280.51
7	26 560.09	1.41e−02	55.97	325.81	276.13
8	26 559.72	1.06e−02	54.70	203.57	25.150
9	26 560.77	8.38e−03	55.43	266.30	75.050
10	26 560.02	1.45e−02	53.36	134.59	65.840
11	26 559.80	2.00e−03	56.10	326.58	147.45
12	26 559.86	1.66e−02	54.46	202.48	232.26
13	26 559.18	5.72e−03	55.19	79.740	64.400
14	26 559.54	1.06e−02	54.72	261.70	56.850
15	26 560.12	1.18e−02	56.66	23.120	53.360
16	26 560.35	1.32e−02	53.52	197.47	48.460
17	26 560.20	1.06e−02	55.60	322.15	38.130
18	26 560.53	6.04e−03	53.61	203.00	209.29
19	26 559.04	2.79e−03	56.62	22.640	304.45
20	26 560.93	2.42e−03	54.72	141.08	112.11
21	26 561.43	4.25e−03	55.93	82.280	58.760
22	26 559.49	7.33e−03	53.62	258.80	20.820
23	26 559.72	7.71e−03	55.09	320.89	7.6900
24	26 560.45	8.28e−03	55.92	82.170	217.98
25	26 560.31	6.36e−03	54.94	141.77	229.63
26	26 561.03	2.16e−03	55.12	144.23	187.36
27	26 560.76	2.95e−03	55.74	23.410	183.78
28	26 559.91	2.83e−03	55.64	80.650	180.09
29	26 560.21	2.42e−03	54.48	264.26	191.16
30	26 560.21	8.79e−04	55.25	25.270	207.44

and considering the servicer initially located at orbit 0 (see Table 2). The fuel mass depletion and the time of flight are computed by using Eq. (22) and Algorithm 4.

It can be observed that the computational time does not present significant variations when the number of considered satellites increases. The MILP algorithm is very fast if coupled with an analytic distance metric. The fuel consumption and the time of flight significantly increase when satellites 3, 4, and 5 are considered. Note that satellites 3, 4, and 5 have a RAAN which significantly differs from those of the satellites previously considered. This behavior is consistent with the fact that RAAN correction requires a large amount of fuel.

Not all of the clients can be visited by the considered servicer spacecraft (satellites that cannot be reached are reported in strike-through). In particular, if client 8 is included in the dataset, the total Δm required to visit all clients is greater than m_{fuel}. The result strictly depends on the initial orbit of the servicer and the clients included in the dataset.

Fig. 4 shows the feasible servicer fuel mass consumption and the time of flight of the optimal sequences reported in Table 3 (i.e., the servicer sequentially visits the satellites until all of the available fuel is depleted). The fuel mass depletion increases when more satellites are included in the dataset, as does the number of clients that can be visited. The servicer depletes almost all the available fuel when more than 7 clients are considered; if new clients are included, they can be reached only if their orbital elements have small differences from those already present in the dataset.

The dependence on the initial state of the servicer is shown in Fig. 5. In this analysis, the full dataset is considered. In each simulation, the initial servicer orbit is swapped with one of the clients' orbits. For example, if the servicer's initial orbit corresponds to the one of client 1, then client 1's initial orbit is changed to orbit 0, and so on. Fig. 5(a) shows the number of clients that can be visited. On the x-axis, the servicer initial orbit ID is reported referring to Table 2. The results are obtained by solving the STSP for all possible permutations. Once the optimal sequence is obtained, the servicer sequentially visits as

Table 3
Optimal sequence, total ΔV, Δm, TOF and CPU time of $\Delta V_{Ed,\Omega}$ using MILP.

N_{sat}	Optimal sequence	$\Delta V_{Ed,\Omega}$ (km/s)	Δm (kg)	TOF (days)	CPU time (s)
1	{0,1}	5.8961	363.21	248.18	2.97e−02
2	{0,2,1}	5.9800	367.87	251.27	3.12e−02
3	{0,2,1,3}	13.417	732.46	500.88	3.12e−02
4	{0,2,1,4,3}	17.809	908.21	620.65	1.56e−02
5	{0,2,1,4,5,3}	19.499	969.17	661.57	9.38e−02
6	{0,2,1,6,4,5,3}	19.532	970.31	662.35	1.56e−02
7	{0,2,1,6,4,5,7,3}	19.583	972.11	663.54	1.56e−02
8	{0,2,8,3,7,5,4,6,1}	19.064	953.83	650.91	2.32e−02
9	{0,2,8,9,3,7,5,4,6,1}	19.087	954.64	651.45	4.58e−02
10	{0,2,10,1,6,4,5,7,3,9,8}	19.932	984.23	671.50	2.41e−02
11	{0,2,10,1,6,4,5,11,7,3,9,8}	19.935	984.32	671.57	3.12e−02
12	{0,2,10,1,6,4,5,11,7,3,9,8,12}	19.935	984.32	671.57	2.87e−02
13	{0,2,10,13,1,6,4,5,11,7,3,9,8,12}	20.095	989.85	675.22	1.58e−02
14	{0,2,10,13,1,6,4,5,11,7,3,9,14,8,12}	20.095	989.85	675.22	3.12e−02
15	{0,2,10,13,1,15,6,4,5,11,7,3,9,14,8,12}	20.234	994.61	678.39	4.69e−02
16	{0,2,10,13,1,15,6,4,5,11,7,3,9,14,8,12,16}	20.234	994.61	678.39	3.12e−02
17	{0,2,10,13,1,15,6,4,5,11,7,17,3,9,14,8,12,16}	20.292	996.57	679.69	1.56e−02
18	{0,2,10,13,1,15,6,4,5,11,7,17,3,9,14,8,18,12,16}	20.292	996.57	679.69	1.56e−02
19	{0,2,10,13,1,15,19,6,4,5,11,7,17,3,9,14,8,18,12,16}	20.293	996.61	679.71	3.12e−02
20	{0,2,20,10,13,1,15,19,6,4,5,11,7,17,3,9,14,8,18,12,16}	20.302	996.93	679.93	4.69e−02
21	{0,2,20,10,21,13,1,15,19,6,4,5,11,7,17,3,9,14,8,18,12,16}	20.378	999.50	681.64	1.56e−02
22	{0,2,20,10,21,13,1,15,19,6,4,5,11,7,17,3,9,14,22,8,18,12,16}	20.378	999.50	681.64	1.56e−02
23	{0,2,20,10,21,13,1,15,19,6,4,5,11,7,17,23,3,9,14,22,8,18,12,16}	20.307	997.08	679.98	1.56e−02
24	{0,2,20,10,21,24,13,1,15,19,6,4,5,11,7,17,23,3,9,14,22,8,18,12,16}	20.307	997.09	679.99	1.56e−02
25	{0,2,25,20,10,21,24,13,1,15,19,6,4,5,11,7,17,23,3,9,14,22,8,18,12,16}	20.311	997.22	680.07	1.56e−02
26	{0,2,26,25,20,10,21,24,13,1,15,19,6,4,5,11,7,17,23,3,9,14,22,8,18,12,16}	20.312	997.25	680.09	3.25e−02
27	{0,2,26,25,20,10,21,24,13,1,27,15,19,6,4,5,11,7,17,23,3,9,14,22,8,18,12,16}	20.367	999.12	681.36	1.56e−02
28	{0,2,26,25,20,10,21,24,28,13,1,27,15,19,6,4,5,11,7,17,23,3,9,14,22,8,18,12,16}	20.370	999.23	681.43	3.12e−02
29	{0,2,26,25,20,10,21,24,28,13,1,27,15,19,6,4,5,11,7,17,23,3,9,29,14,22,8,18,12,16}	20.370	999.23	681.43	1.56e−02
30	{0,2,26,25,20,10,21,24,28,13,1,30,27,15,19,6,4,5,11,7,17,23,3,9,29,14,22,8,18,12,16}	20.390	999.93	681.88	1.56e−02

many clients as possible before running out of fuel. If the full dataset is considered, the servicer can visit between 19 and 23 clients. This result does not contradict those reported in Table 3. The number of visited clients strictly depends on the orbits considered in the dataset. In fact, considering the servicer initially located in orbit 0, the first 22 clients can be visited if the full dataset is considered, while only 7 clients can be visited if the dataset includes only the first 8 satellites (see Table 3). Fig. 5(b) shows the fuel mass depletion and the time of flight required for each possible permutation. It is visible how the number of visited clients is maximum when the servicer depletes almost all the available fuel. In a few cases, the servicer fuel mass depletion is about 150 kg lower than m_{fuel}. In those cases, reaching the next client of the associated optimal sequence would require more than the remaining fuel. A very low computational burden is associated with the analysis shown in Fig. 5. All simulations, including the computation of weights using the selected distance metric, were completed in less than 1 second.

It is important to note that this analysis focused on finding the minimum ΔV associated with a complete tour, and the fuel mass constraints were subsequently evaluated based on this solution. While this approach does not directly address the problem of maximizing the number of visitable targets under fuel constraints, it efficiently provides a lower bound on the number of satellites that can be visited. This lower bound is obtained with minimal computational effort, offering a fast and practical approximation for mission planning.

6.1.1. Error analysis incorporating phasing maneuvers

To evaluate the amount of error in the solutions arising from neglecting rendezvous costs (Assumption 3), the cost of rendezvous maneuvers is estimated using the analytical approach presented in Ref. [20]. This approach calculates the ΔV required for phasing between two satellites sharing the same orbit. This phasing maneuver involves adjusting the orbital period to correct the true anomaly difference, $\Delta\theta$, with the associated ΔV cost expressed as

$$\Delta V_{RV} = \frac{4a_0}{3}\frac{\Delta\theta}{\Delta t_{RV}} \tag{23}$$

where a_0 is the semi-major axis of the orbit, and Δt_{RV} is the time allocated for the phasing maneuver.

The optimal sequence results in Fig. 5 were analyzed under the worst-case condition $\Delta\theta = \pi$ rad. This scenario assumes that for all visits, the servicer must correct the true anomaly difference $\Delta\theta$ at the end of the orbit change maneuver, with phasing durations in the range $\Delta t_{RV} \in [5, 10]$ days.

Fig. 6 shows the percentage errors in total mass depletion and total time of flight for the most and least fuel-demanding sequences. These correspond to the optimal sequences where the servicer initiates its trajectory from orbits 2 and 10, respectively (see Fig. 5).

The analysis demonstrates that phasing duration affects fuel consumption. Shorter phasing times require larger semi-major axis adjustments to achieve the necessary passive drift rate, resulting in higher fuel costs. Conversely, longer phasing durations lower fuel costs but increase the total time of flight. It is important to emphasize that the presented results reflect an extreme case, where phasing maneuvers constitute a separate stage of the trajectory. In more typical scenarios, where, on average, the angular separation is smaller and phasing occurs as part of the trajectory itself, the overall cost of the phasing maneuver is reduced.

6.2. Molnyia constellation test case

For eccentric orbits, no analytic solutions exist to quantify the cost of a transfer maneuver for a simultaneous correction of five orbital elements using low-thrust. In this case, the ΔV_{QL} distance metric is employed to provide appropriate weights for both minimum-time and minimum-fuel frameworks to solve the combinatorial problem. The algorithm was applied to a set of 42 high-eccentricity orbits taken from a Molnyia constellation. Table 4 reports the initial Keplerian elements of the satellites [34] (notice that the sixth orbital elements is used only for error assessment in the next section).

Q-law weights (W_P, W_i) and stopping criteria tolerances (ϵ_i) used in the simulations are reported in Table 5 (a_f and e_f indicate that stopping criteria tolerances on semi-major axis and eccentricity were

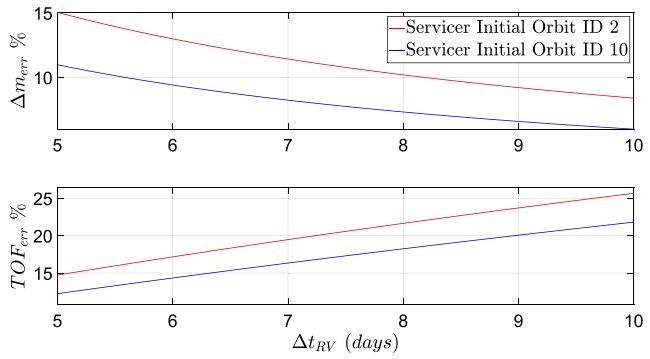

Fig. 6. Phasing maneuver cost error estimation.

set as a percentage of the targeted values). In the case of minimum-fuel Q-law, the relative and absolute effectivity thresholds were set as $\overline{\eta}_r = 0.2$ and $\overline{\eta}_a = 0.2$. These parameters were selected by a trial-and-error procedure on a sample transfer maneuver. They proved to be a good choice in terms of Q-law convergence computational time. In principle, they could be optimized for each possible transfer at the expense of an increased computational burden. Q-law was integrated using adaptive Runge–Kutta 78 with a relative tolerance of 1×10^{-7}. The initial servicer orbit was considered to be at the orbit 0 of the set.

The weights computation required 861 system integrations for each case. The ΔV required for each possible transfer is shown in Fig. 7 as obtained for the minimum-time case.

From Fig. 7, it can be noted that most expensive maneuvers require a ΔV of about 10 km/s. In particular, orbits 6, 20 and 41 are the most expensive to target or to depart from.

Once the ΔVs are computed, the MILP is used to find the optimal sequence. The results for both minimum-time and minimum-fuel case are reported in Table 6 in terms of optimal sequence, total ΔV, total fuel mass consumption, total time of flight and computational time.

Notably, the servicer successfully visits all clients with the onboard fuel. This highlights how low-thrust propulsion, in general, enables the visitation of a larger number of orbits, albeit with longer time of flights. Furthermore, it is notable that the optimal sequences are slightly different for the two simulations (i.e., orbits 20 and 6 are switched). This behavior is due to the fact that the coast arc mechanism (and consequently the ΔV) depends on the servicer trajectory which depends on the departure orbit (i.e., the ΔV required for a transfer maneuver in the minimum-time case is not linearly proportional to the one required in the minimum-fuel case for each possible transfer). Additionally, as expected, in the minimum-fuel case, the servicer visits all clients by saving about 80 kg in fuel but requiring about 64 days more than the minimum-time results. This aspect may have an impact on operational constraints, giving more insights on the mission feasibility and affordability. In contrast, the computational time required by the minimum-fuel simulation is about 2.6 times longer than the one required by the minimum-time scenario. This is consistent with the additional time required for the effectivities evaluation as discussed in Section 3.2.

As a final note, the computational time of the MILP/Q-law is several orders of magnitude higher compared to the test case in Section 6.1. This discrepancy arises because calculating transfer costs using the Q-law for eccentric orbits involves system integration, instead of a simple function evaluation. This highlights the importance of selecting an appropriate distance metric based on the specific orbital characteristics of the dataset, as it influences both the accuracy of cost estimates and the computational time for weight calculations. Despite this increased computational complexity, the MILP algorithm efficiently handles the combinatorial problem, with the optimal sequence determined in under 1 second across all simulations.

Table 4
Molnyia constellation servicer and clients initial Keplerian elements.

ID	a (km)	e	i (deg)	Ω (deg)	ω (deg)	θ (deg)
0	26 580.72	7.37e−01	63.40	310.28	282.57	46.62
1	26 574.82	7.22e−01	64.13	355.47	274.96	29.77
2	26 579.70	7.43e−01	62.85	318.66	280.43	180.0
3	26 578.61	7.39e−01	63.08	288.70	281.34	236.7
4	26 578.36	7.43e−01	62.94	300.76	280.33	34.75
5	26 574.90	7.42e−01	62.87	289.39	280.33	32.90
6	26 640.38	6.90e−01	63.56	134.46	276.29	158.7
7	26 579.66	7.41e−01	62.87	310.63	280.30	100.9
8	26 574.08	7.42e−01	62.80	307.57	280.11	32.24
9	26 576.84	7.43e−01	62.87	300.43	280.31	29.65
10	26 577.93	7.45e−01	62.83	5.5700	280.34	30.30
11	26 574.82	7.44e−01	62.88	19.940	280.55	31.75
12	26 571.71	7.44e−01	62.83	49.460	279.94	21.41
13	26 579.59	7.43e−01	62.85	313.41	280.27	7.05
14	26 579.28	7.43e−01	62.85	42.710	280.34	31.66
15	26 579.77	7.40e−01	62.91	311.83	281.08	35.25
16	26 577.53	7.41e−01	62.86	322.50	279.82	47.03
17	26 579.56	7.42e−01	62.85	46.270	280.17	31.89
18	26 573.94	7.43e−01	62.89	349.73	280.17	43.42
19	26 646.00	7.11e−01	63.50	257.10	282.29	37.60
20	26 997.02	6.86e−01	63.81	143.51	272.19	229.6
21	26 579.59	7.42e−01	62.86	341.38	280.38	231.3
22	26 579.95	7.40e−01	62.85	303.47	280.63	73.26
23	26 573.25	7.41e−01	62.87	324.17	280.39	74.95
24	26 579.50	7.42e−01	62.87	326.26	280.24	63.96
25	26 579.75	7.42e−01	62.87	306.26	280.46	57.29
26	26 571.85	7.42e−01	63.06	300.55	280.30	49.52
27	26 579.98	7.42e−01	63.00	335.96	280.15	54.88
28	26 575.88	7.42e−01	62.86	314.71	280.84	48.33
29	26 576.78	7.38e−01	62.92	289.56	281.95	51.18
30	26 578.37	7.43e−01	62.90	352.12	280.51	49.67
31	26 579.98	7.42e−01	62.85	243.44	280.31	62.80
32	26 579.97	7.42e−01	62.86	269.96	280.45	64.94
33	26 577.28	7.43e−01	62.83	241.84	280.42	254.3
34	26 575.27	7.41e−01	62.96	329.29	281.60	34.38
35	26 578.62	7.43e−01	62.80	245.40	280.37	53.36
36	26 579.35	7.42e−01	62.89	295.99	280.59	34.50
37	26 579.82	7.43e−01	62.86	275.46	280.28	32.21
38	26 576.12	7.44e−01	62.86	311.80	280.45	27.61
39	26 575.06	7.42e−01	62.86	6.2000	280.33	30.57
40	26 571.97	7.43e−01	62.86	248.91	280.46	190.5
41	26 559.84	7.36e−01	62.86	202.79	288.20	224.0

Table 5
Q-law user-defined parameters.

Parameter	Unit	Value
W_P	–	5
W_i	–	[10,2,2,1,1]
ϵ_1	km	$0.001a_f$
ϵ_2	–	$0.01e_f$
ϵ_3	deg	0.1
ϵ_4	deg	0.1
ϵ_5	deg	0.1

6.2.1. Effect of secular J_2 perturbation and rendezvous cost

In order to assess the accuracy of the solution, some of the assumptions are relaxed, namely Assumptions 2 and 3. In particular, the impact of the secular J_2 perturbations and the rendezvous cost on the optimal sequences is analyzed. Both the servicer and the clients are subject to secular J_2 by adding to Eqs. (1) and (5) the following term [35]

$$\dot{\mathbf{X}}_{J_2}(t) = \begin{bmatrix} \mathbf{0}_{3\times1} \\ -\frac{3}{2} J_2 \sqrt{\frac{\mu}{a(t)^3}} \left(\frac{R_e}{p(t)}\right)^2 \cos\left(i(t)\right) \\ \frac{3}{4} J_2 \sqrt{\frac{\mu}{a(t)^3}} \left(\frac{R_e}{p(t)}\right)^2 \left(5\cos^2\left(i(t)\right) - 1\right) \\ \mathbf{0}_{2\times1} \end{bmatrix} \tag{24}$$

where $J_2 = 1.083 \times 10^{-3}$ is the first zonal harmonic coefficient, and $R_e = 6378.137$ km is the Earth equatorial radius. The rendezvous cost is

Table 6
Optimal sequence, total ΔV, Δm, TOF and CPU time of Q-law using MILP.

	Optimal sequence	ΔV (km/s)	Δm (kg)	TOF (days)	CPU time (s)
Minimum-time	{0,15,7,38,13,28,2,16,23,24,34,27,21,18, 30,1,10,39,11,14,17,12,20,6,41,33,31, 35,40,19,32,37,5,3,29,36,9,26,4,22,25,8}	17.26	887.79	604.60	1215.4
Minimum-fuel	{0,15,7,38,13,28,2,16,23,24,34,27,21,18, 30,1,10,39,11,14,17,12,6,20,41,33,31, 35,40,19,32,37,5,3,29,36,9,26,4,22,25,8}	15.18	806.09	668.48	3158.7

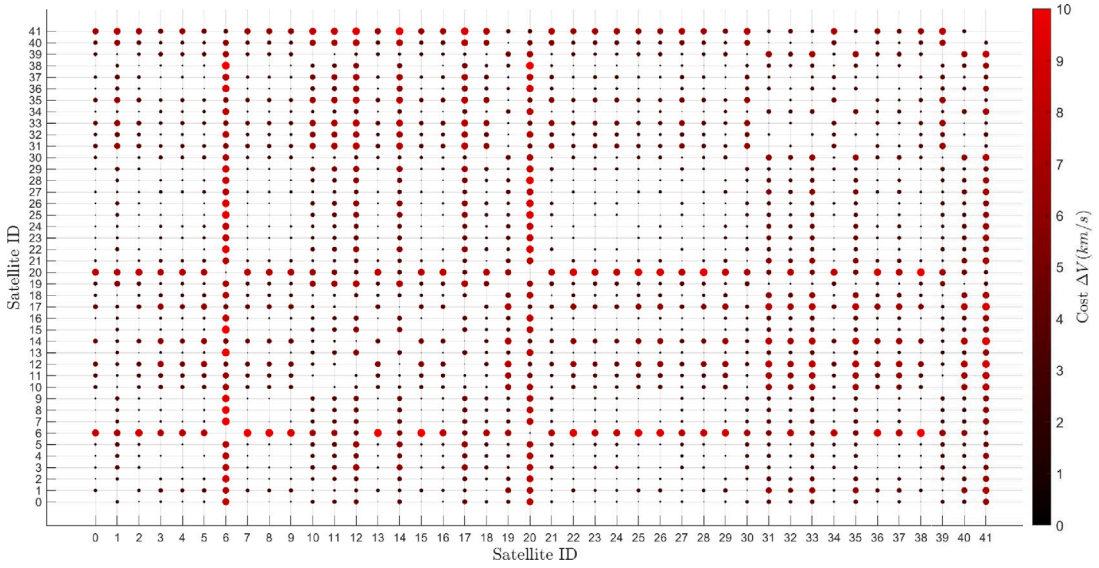

Fig. 7. ΔV computed by the Q-law (minimum-time).

evaluated by adopting a modified Q-law as developed in Ref. [36]. The fast variable targeting is assessed by introducing an additional error in the semi-major axis target state. The error state assumes the following form

$$\hat{\mathbf{Z}}(t) = \begin{bmatrix} a(t) - \hat{a}_T(t) \\ e(t) - e_T \\ i(t) - i_T \\ \arccos\left(\cos\left(\Omega(t) - \Omega_T(t)\right)\right) \\ \arccos\left(\cos\left(\omega(t) - \omega_T(t)\right)\right) \end{bmatrix} \tag{25}$$

where the time dependence of the servicer and the target orbital state is underlined and

$$\hat{a}_T(t) = a_T + \frac{2W_L}{\pi}\left(a_T - \frac{r_{p,min}}{1-e(t)}\right)\arctan\left(W_{scl}\Delta L(t)\right). \tag{26}$$

In Eq. (26), $r_{p,min} = 6578$ km is the minimum perigee distance, $W_L = 6\times10^{-2}$ and $W_{scl} = 0.7$ are two additional user-defined parameters. The term ΔL is the difference in true longitude between the servicer and the client wrapped to the range $[-\pi, \pi]$ and it is defined as

$$\begin{aligned}\Delta L(t) &= L(t) - L_T(t) \\ &= \omega(t) + \Omega(t) + \theta(t) - \omega_T(t) - \Omega_T(t) - \theta_T(t).\end{aligned}$$

The control acceleration form remains unchanged with the difference that the term $\partial Q(\mathbf{Z})/\partial \mathbf{Z}$ is evaluated at $\hat{\mathbf{Z}}(t)$. When rendezvous is considered, the Q-law is integrated until the orbital elements differ less than the stopping criteria reported in Table 5 and $\arccos(\cos(\Delta L)) \leq 0.1$ deg.

An example of a six-orbital-element targeting trajectory computed by including the effect of secular J_2 is shown in Fig. 8 for the minimum-time case. The servicer, departing from orbit 12 (yellow line) performs a rendezvous with the client located at orbit 20. The effect of secular J_2 is highlighted by the client orbit propagation (in magenta). The final positions of the servicer and the client are shown respectively with a green dot and a red square.

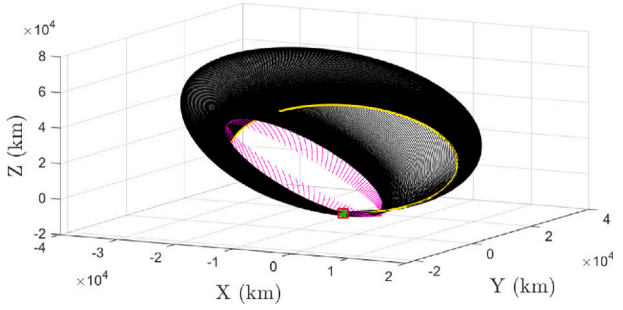

Fig. 8. Trajectory with secular J_2 and rendezvous from orbit 12 to orbit 20. (For interpretation of the references to color in this figure legend, the reader is referred to the web version of this article.)

It is important to note that Eq. (26) enables the phasing maneuver to be executed throughout the entire transfer, allowing both the orbital transfer and phasing to occur simultaneously. This approach eliminates the need to separate these phases.

The optimal sequences previously found have been evaluated by considering Eqs. (24), (25) and (26). The same propulsion system and Q-law user-defined parameters as reported in Tables 1 and 5 are adopted.

The absolute percentage errors for both total fuel consumption and total time of flight have been computed as follows

$$ERR_{\Delta m} = \frac{|\Delta m_{val} - \Delta m_{QL}|}{\Delta m_{val}} \times 100$$

$$ERR_{TOF} = \frac{|TOF_{val} - TOF_{QL}|}{TOF_{val}} \times 100$$

Table 7
Total ΔV, Δm, TOF and errors with secular J_2 and rendezvous.

	ΔV (km/s)	Δm (kg)	TOF (days)	$ERR_{\Delta m}$ (%)	ERR_{TOF} (%)
Minimum-time RV	17.83	908.87	618.96	2.32	2.32
Minimum-time J_2	17.47	895.68	609.98	0.88	0.88
Minimum-time RV J_2	17.87	910.61	620.14	2.51	2.51
Minimum-fuel RV	15.23	808.12	683.22	0.25	2.16
Minimum-fuel J_2	15.40	814.91	712.08	1.08	6.12
Minimum-fuel RV J_2	15.54	816.88	727.19	1.32	8.07

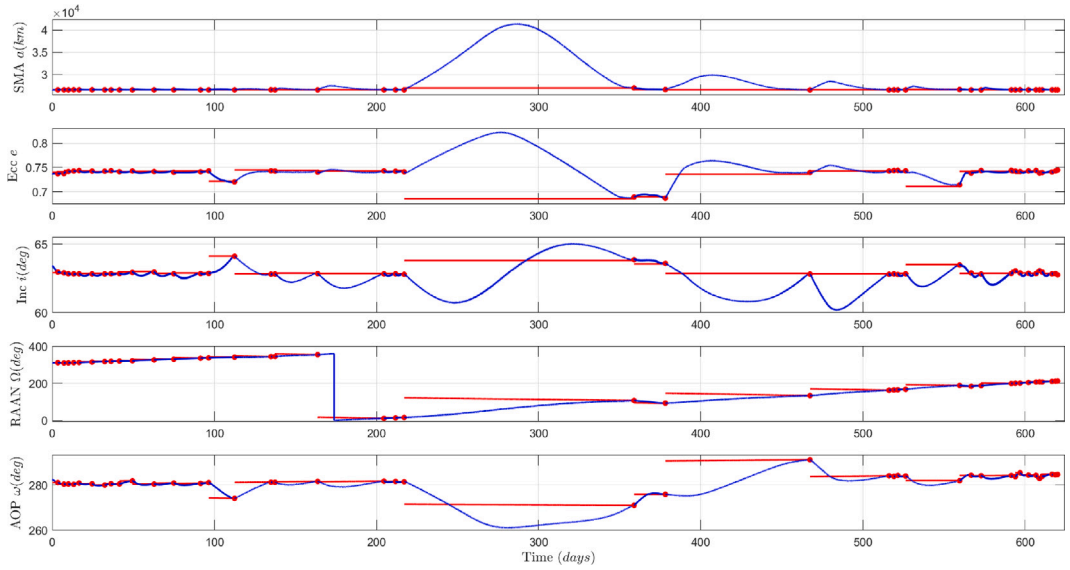

Fig. 9. Optimal sequence orbital elements history (minimum-time), incorporating secular J_2 and rendezvous. (For interpretation of the references to color in this figure legend, the reader is referred to the web version of this article.)

where Δm_{val} and TOF_{val} refer to the results obtained by including secular J_2 effect and rendezvous cost while Δm_{QL} and TOF_{QL} refer to the results reported in Table 6. Table 7 reports the results in terms of total ΔV, Δm, TOF and the errors as obtained by evaluating the optimal sequences found by the MILP/Q-law algorithm and including rendezvous cost (denoted as RV) and the secular J_2 effect. The errors have been evaluated by separating the effect of rendezvous only, the secular J_2 only, and both rendezvous and secular J_2.

As expected, the servicer fuel consumption increases if the rendezvous maneuver is performed. Nevertheless, the additional amount of fuel required is a small percentage of the total fuel consumption (less than 3% errors for both the minimum-time and minimum-fuel case). Notably, the effect of secular J_2 increases both the fuel consumption and the time of flight. Clients' orbits are precessing in a way to increase the difference in orbital elements that the servicer must correct (i.e., clients' orbits are drifting apart). In the minimum-time case, this effect has a low impact on both the fuel mass consumption and time of flight (less than 3% errors). On the other hand, the percentage error in the time of flight increases for the minimum-fuel framework (the longer the time to visit all the satellites, the greater the drift due to secular J_2). However, due to the non-linear proportionality between fuel consumption and time of flight, the fuel consumption percentage error is less than 2%. When both the effect of secular J_2 and rendezvous cost are combined, the percentage errors increase. The fuel consumption errors are less than 3% while the time of flight percentage errors are mainly affected by the effect of secular J_2.

Fig. 9 shows the time history of the servicer's orbital elements for the optimal sequence in the minimum-time case when both secular J_2 and rendezvous are considered. The servicer trajectory is shown with a blue line, the client trajectories are in red, and the rendezvous instants are indicated by a red dot.

The arguments of perigee for the client satellites remain nearly constant. Molnyia orbit inclination is chosen such that $i \sim \arccos(\sqrt{1/5}) = 63.4349$ deg in order to have $\dot{\omega} \sim 0$ (see Eq. (24)). The effect of RAAN precession is more pronounced, especially for maneuvers requiring long time of flights. The orbital planes of the clients rotate counterclockwise ($\dot{\Omega} < 0$). Notably, for most of the maneuvers it appears that RAAN precession decreases the difference in RAAN the servicer must correct. This result is not in contrast to what is reported in Table 7. In fact, the effect on the individual leg does not reflect the trend on all satellites in the dataset (i.e., clients are drifting with respect to each other, increasing the mutual distance among them). Elongations of the semi-major axis and eccentricities are present, mainly in the last phase of the tour. This behavior characterizes the Q-law feedback controller [27] and typically is present when the maneuver requires a large correction of the RAAN. Changing Ω and i is cheaper when the satellite is maneuvered at greater semi-major axis. In order to minimize the time needed to enlarge the orbit, the controller increases the eccentricity exploiting the apogee phases to steer the thrust with a greater out-of-plane component which mainly acts on RAAN and inclination changes. The Ω history plot indicates that clients are visited following an almost ascending orbit plane rotation with respect to servicer initial RAAN. This behavior, called *RAAN walk* [14], is consistent with the fact that RAAN correction requires a large amount of fuel.

As a final remark, for Molnyia orbits, the altitude of the perigee may present certain criticalities due to the high eccentricity of these orbits. The osculating altitude of the perigee during the trajectory illustrated in Fig. 9 is calculated as $h_p(t) = r_p(t) - R_e$, where $r_p(t) = a(t)(1 - e(t))$ represents the perigee distance of the osculating trajectory. Fig. 10 shows the perigee altitude and compares it to the limit established in Eq. (26), where the minimum perigee altitude is $h_{p,min} = r_{p,min} - R_e = 199.86$ km. The trajectory remains above this limit, ensuring a feasible trajectory.

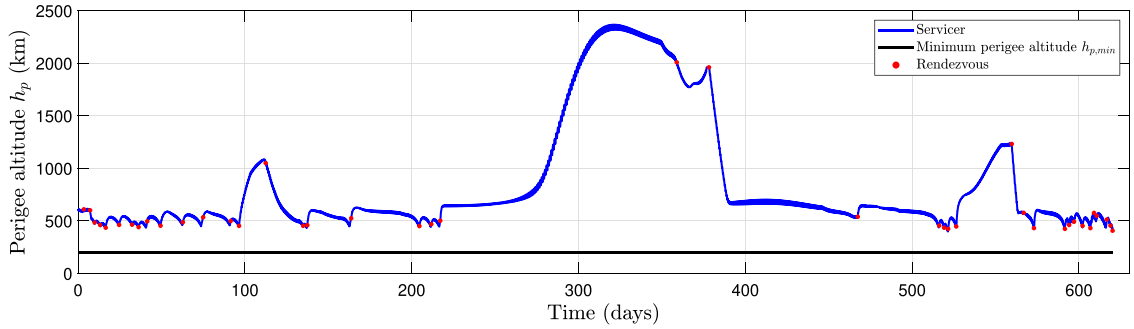

Fig. 10. Minimum perigee altitude validation.

7. Conclusions

In this article, we have solved the problem of optimal tour planning for a low-thrust, multiple-visitation, satellite-servicing problem. Two distance metrics are used to quantify the cost of orbit-to-orbit maneuvers. The first is based on an analytic function derived using Edelbaum's theory; it accounts for circular-to-circular transfer. The second exploits the Q-law feedback controller to derive a near-optimal ΔV distance metric. The globally optimal visiting sequence is obtained by MILP.

The performance of the proposed approach has been tested on two different datasets of satellites located in the MEO region. The first test case considered up to thirty-one near-circular orbits taken from the GPS constellation. The results are found in extremely low computational times by adopting the analytic distance metric. The dependence of the optimal solution on the dataset size and initial orbit of the servicer spacecraft is also analyzed. The second test case considers up to 42 high-eccentricity orbits taken from a Molnyia constellation. The Q-law based distance metric is adopted. The optimal sequence is found for both minimum-time and minimum-fuel cases. The accuracy of the results is assessed by including the secular J_2 effect and rendezvous costs. The absolute errors in total fuel consumption and time of flight are less than 3% for the minimum-time case. The secular J_2 effect has a larger impact in terms of total time of flight for the minimum-fuel case (about 8%).

The novelty of coupling the Q-law based distance metric and MILP resulted in a fast and versatile algorithm. Key aspects include the possibility to have five-orbital-element targeting maneuver cost estimations (both minimum-time and minimum-fuel) to find an optimal sequence, to reconstruct the entire trajectory and control law within the algorithm, and to obtain information such as fuel mass depletion and time of flight. Despite the focus on the challenging case of low-thrust propulsion, the proposed methodology is equally applicable to open tour planning for missions employing high-thrust propulsion, provided that the underlying assumptions of the model hold, while maintaining the same computational complexity. Furthermore, the proposed methodology can be applied to a general client satellite dataset with arbitrary orbital elements.

The proposed approach might perform poorly for highly perturbed environments, such as LEO, especially in terms of a loss of accuracy of the optimal solution. In fact, when perturbations are significant, the distance metric becomes time-dependent, represented as $\Delta V(d_i, d_j, t_{0,k})$, with $t_{0,k}$ denoting the departure time of the transfer maneuver.

Overall, the proposed algorithm represents a fast and accurate solution to assess the trajectory design and feasibility of multiple-visitation missions.

CRediT authorship contribution statement

Riccardo Apa: Writing – review & editing, Writing – original draft, Validation, Software, Methodology, Conceptualization. **Isaac Kaminer:** Writing – review & editing, Validation. **Jennifer Hudson:** Writing – review & editing, Validation, Conceptualization. **Marcello Romano:** Writing – review & editing, Validation, Conceptualization.

Declaration of competing interest

The authors declare that they have no known competing financial interests or personal relationships that could have appeared to influence the work reported in this paper.

Acknowledgments

This research is part of the project NODES which has received funding from the MUR – M4C2 1.5 of PNRR funded by the European Union - NextGenerationEU (Grant agreement no. ECS00000036), and part of a grant of Compagnia di San Paolo.

References

[1] In-Space Servicing, Assembly, and Manufacturing Interagency Working Group of the National Science & Technology Council, In-space servicing, assembly and manufacturing national strategy, 2022.

[2] Johannes Schneider, The time-dependent traveling salesman problem, Phys. A 314 (1–4) (2002) 151–155, http://dx.doi.org/10.1016/S0378-4371(02)01078-6.

[3] Dalal Madakat, Jérôme Morio, Daniel Vanderpooten, Biobjective planning of an active debris removal mission, Acta Astronaut. 84 (2013) 182–188, http://dx.doi.org/10.1016/j.actaastro.2012.10.038.

[4] M. Cerf, Multiple space debris collecting mission—Debris selection and trajectory optimization, J. Optim. Theory Appl. 156 (3) (2013) 761–796, http://dx.doi.org/10.1007/s10957-012-0130-6.

[5] Dario Izzo, Marcus Märtens, The kessler run: On the design of the GTOC9 challenge, Acta Futura 11 (1) (2018) 11–24.

[6] Brent William Barbee, Salvatore Alfano, Elfego Piñon, Kenn Gold, David Gaylor, Design of spacecraft missions to remove multiple orbital debris objects, in: 2011 Aerospace Conference, 2011, pp. 1–14, http://dx.doi.org/10.1109/AERO.2011.5747303.

[7] Zhong Zhang, Nan Zhang, Yifei Jiao, Hexi Baoyin, Junfeng Li, Multitree search for multisatellite responsiveness scheduling considering orbital maneuvering, IEEE Trans. Aerosp. Electron. Syst. 58 (3) (2022) 2206–2217, http://dx.doi.org/10.1109/TAES.2021.3129723.

[8] Sanjeev Narayanaswamy, Benjamin Wu, Philippe Ludivig, Frank Soboczenski, Karthik Venkataramani, Christopher J. Damaren, Low-thrust rendezvous trajectory generation for multi-target active space debris removal using the RQ-law, Adv. Space Res. 71 (10) (2023) 4276–4287, http://dx.doi.org/10.1016/j.asr.2022.12.049.

[9] Haiyang Li, Shiyu Chen, Hexi Baoyin, J2-perturbed multitarget rendezvous optimization with low thrust, J. Guid. Control Dyn. 41 (3) (2018) 802–808, http://dx.doi.org/10.2514/1.G002889.

[10] Giacomo Gatto, Lorenzo Casalino, Fast evaluation and optimization of low-thrust transfers to multiple targets, J. Guid. Control Dyn. 38 (8) (2015) 1525–1530, http://dx.doi.org/10.2514/1.G001116.

[11] Federico Zuiani, Massimiliano Vasile, Preliminary design of debris removal missions by means of simplified models for low-thrust, many-revolution transfers, Int. J. Aerosp. Eng. 2012 (2012) 1–22, http://dx.doi.org/10.1155/2012/836250.

[12] Marilena Di Carlo, Juan Manuel Romero Martin, Massimiliano Vasile, Automatic trajectory planning for low-thrust active removal mission in low-earth orbit, Adv. Space Res. 59 (5) (2017) 1234–1258, http://dx.doi.org/10.1016/j.asr.2016.11.033.

[13] Zhao Wei, Teng Long, Renhe Shi, Yufei Wu, Nianhui Ye, Scheduling optimization of multiple hybrid-propulsive spacecraft for geostationary space debris removal missions, IEEE Trans. Aerosp. Electron. Syst. 58 (3) (2022) 2304–2326, http://dx.doi.org/10.1109/TAES.2021.3131294.

[14] Dario Izzo, Ingmar Getzner, Daniel Hennes, Luís Felismino Simões, Evolving solutions to TSP variants for active space debris removal, in: Proceedings of the 2015 Annual Conference on Genetic and Evolutionary Computation, ACM, Madrid Spain, 2015, pp. 1207–1214, http://dx.doi.org/10.1145/2739480.2754727.

[15] DongUk Lee, Jaemyung Ahn, Optimal multitarget rendezvous using hybrid propulsion system, J. Spacecr. Rockets 60 (2) (2023) 689–698, http://dx.doi.org/10.2514/1.A35540.

[16] Gábor I. Varga, J.M. Sánchez Pérez, Many-revolution low-thrust orbit transfer computation using equinoctial Q-law including J2 and eclipse effects, in: 6th International Conference on Astrodynamics Tools and Techniques, Vol. 1, Darmstatd Germany, 2016, pp. 29–42.

[17] Max Cerf, Multiple space debris collecting mission: Optimal mission planning, J. Optim. Theory Appl. 167 (1) (2015) 195–218, http://dx.doi.org/10.1007/s10957-015-0705-0.

[18] Theodore N. Edelbaum, Optimum low-thrust rendezvous and station keeping, AIAA J. 2 (7) (1964) 1196–1201, http://dx.doi.org/10.2514/3.2521.

[19] Richard H. Battin, An introduction to the mathematics and methods of astrodynamics, Rev. ed., AIAA education series, American Institute of Aeronautics and Astronautics, 1999.

[20] Theodore N. Edelbaum, Propulsion requirements for controllable satellites, ARS J. 31 (8) (1961) 1079–1089, http://dx.doi.org/10.2514/8.5723.

[21] Jean A. Kéchichian, Analytic representations of optimal low-thrust transfer in circular orbit, in: Bruce A. Conway (Ed.), Spacecraft Trajectory Optimization, first ed., Cambridge University Press, 2010, pp. 139–177, http://dx.doi.org/10.1017/CBO9780511778025.007.

[22] Hong-Xin Shen, Explicit approximation for J2-perturbed low-thrust transfers between circular orbits, J. Guid. Control Dyn. 44 (8) (2021) 1525–1531, http://dx.doi.org/10.2514/1.G005415.

[23] Anastassios E. Petropoulos, Simple control laws for low-thrust orbit transfers, Adv. Astronaut. Sci. 116 (2003) 2031–2047.

[24] Hanspeter Schaub, John L. Junkins, Analytical Mechanics Of Space Systems, American Institute of Aeronautics and Astronautics, Reston ,VA, 2003, http://dx.doi.org/10.2514/4.861550.

[25] D.E. Rutherfobd, Optimal trajectories for space navigation. by d. f. lawden. pp. viii, 126. 21s. net. 1963. (butterworth and co.), Math. Gaz. 48 (366) (1964) 478–479, http://dx.doi.org/10.2307/3611765.

[26] John E. Prussing, Primer vector theory and applications, in: Bruce A. Conway (Ed.), Spacecraft Trajectory Optimization, first ed., Cambridge University Press, 2010-08-23, pp. 16–36, http://dx.doi.org/10.1017/CBO9780511778025.003.

[27] Anastassios E. Petropoulos, Refinements to the Q-law for low-thrust orbit transfers, Adv. Astronaut. Sci. 120 (2005) 963–982.

[28] Jackson L Shannon, Martin T Ozimek, Justin A Atchison, M Christine, Q-law aided direct trajectory optimization for the high-fidelity, many-revolution low-thrust orbit transfer problem, Adv. Astronaut. Sci. 168 (2019) 781–800.

[29] Benjamin Ethan Joseph, Lyapunov Feedback Control in Equinoctial Elements Applied to Low Thrust Control of Elliptical Orbit Constellations (Ph.D. thesis), Massachusetts Institute of Technology, 2006.

[30] Demyan V Lantukh, Christopher L Ranieri, Marc D DiPrinzio, Peter J Edelman, Enhanced Q-law Lyapunov control for low-thrust transfer and rendezvous design, in: 2017 AAS/AIAA Astrodynamics Specialist Conference, 2017.

[31] Juan Pablo Vielma, Mixed integer linear programming formulation techniques, SIAM Rev. 57 (1) (2015) 3–57, http://dx.doi.org/10.1137/130915303.

[32] Chao Han, Sihang Zhang, Xinwei Wang, On-orbit servicing of geosynchronous satellites based on low-thrust transfers considering perturbations, Acta Astronaut. 159 (2019) 658–675, http://dx.doi.org/10.1016/j.actaastro.2019.01.041.

[33] Yuri Shimane, Nicholas Gollins, Koki Ho, Orbital facility location problem for satellite constellation servicing depots, J. Spacecr. Rockets 61 (3) (2024) 808–825, http://dx.doi.org/10.2514/1.A35691.

[34] Elisa Maria Alessi, Alberto Buzzoni, Jérôme Daquin, Albino Carbognani, Giacomo Tommei, Dynamical properties of the molniya satellite constellation: Long-term evolution of orbital eccentricity, Acta Astronaut. 179 (2021) 659–669, http://dx.doi.org/10.1016/j.actaastro.2020.11.047.

[35] Vladimir A. Chobotov (Ed.), Orbital mechanics, third. ed, AIAA education series, American Institute of Aeronautics and Astronautics, Reston, Va, 2002.

[36] Sanjeev Narayanaswamy, Christopher J. Damaren, Equinoctial Lyapunov control law for low-thrust rendezvous, J. Guid. Control Dyn. 46 (4) (2023-04) 781–795, http://dx.doi.org/10.2514/1.G006662.